Electronic Supplementary Material (ESI) for Journal of Materials Chemistry A.

Supporting Information

Room Temperature Synthesis and Pressure-Induced Optical Properties of Lead-Free 2D $Cs_3Bi2I_6Cl_3$ Perovskite Nanocrystals

Jie Zhang,* Mingxing Li, Dehua Wang, Binhua Chu, Shufang Zhang, Qinfeng Xu, and Kai Wang*

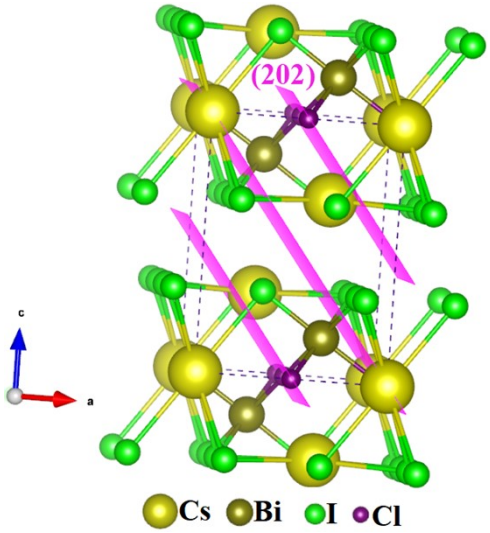

Figure S1. The solved crystal structure of $Cs_3Bi_2I_6Cl_3$ viewed from the b-axis upwards under ambient conditions, intuitively showing the crystal planes of (202).

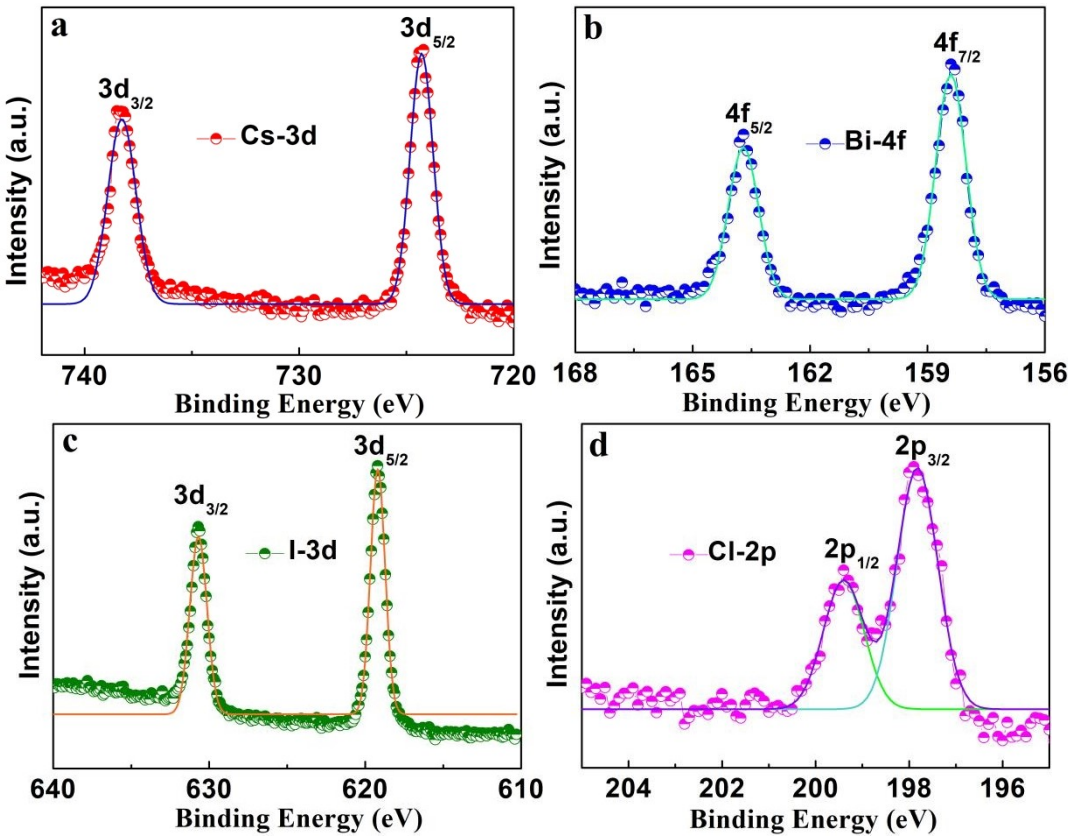

Figure S2. High-resolution XPS spectra and peak fitting for: (a) Cs^+, the peaks at 738.5 and 724.2 eV correspond to the 3d doublet of Cs^+, (b) Bi^{3+}, the peaks at 163.7 and 158.4 eV correspond to the $4f_{5/2}$ and $4f_{7/2}$ levels of Bi^{3+}, (c) I^-, the peaks at 630.7 and 619.2 eV correspond to the I $3d_{3/2}$ and I $3d_{5/2}$ levels, (d) Cl^-, the peaks at 199.4 and 197.9 eV correspond to the $2p_{1/2}$ and $2p_{3/2}$ levels of Cl^-.

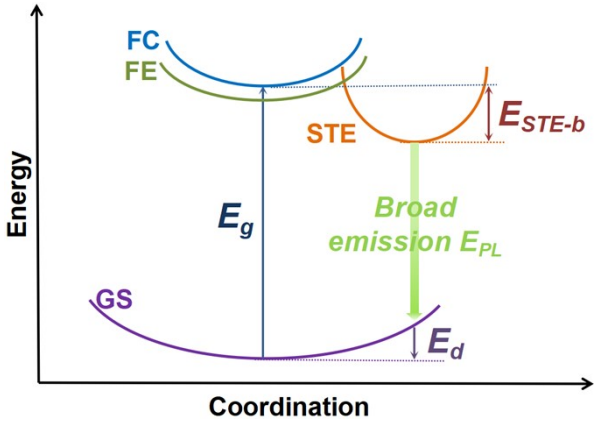

Figure S3. Schematic illustrations of the energy level structure in the STE. Ground state (GS), free carrier state (FC), free exciton state (FE), self-trapped exciton state (STE), bandgap energy (E_g), emission energy (E_{PL}), exciton binding energy of the STE ($E_{STE-\mathrm{b}}$), lattice deformation energy (E_{d}).

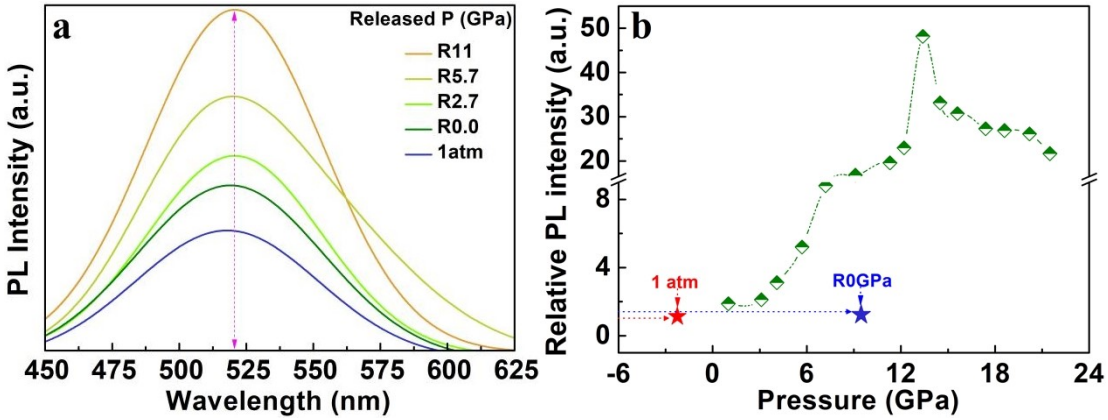

Figure S4. (a) PL emission spectra of $Cs_3Bi_2I_6Cl_3$ NCs under decompression and atmospheric condition for comparison. (b) Relative PL intensity of $Cs_3Bi_2I_6Cl_3$ NCs as a function of pressure. "R" represents PL emission spectra collected on pressure release.

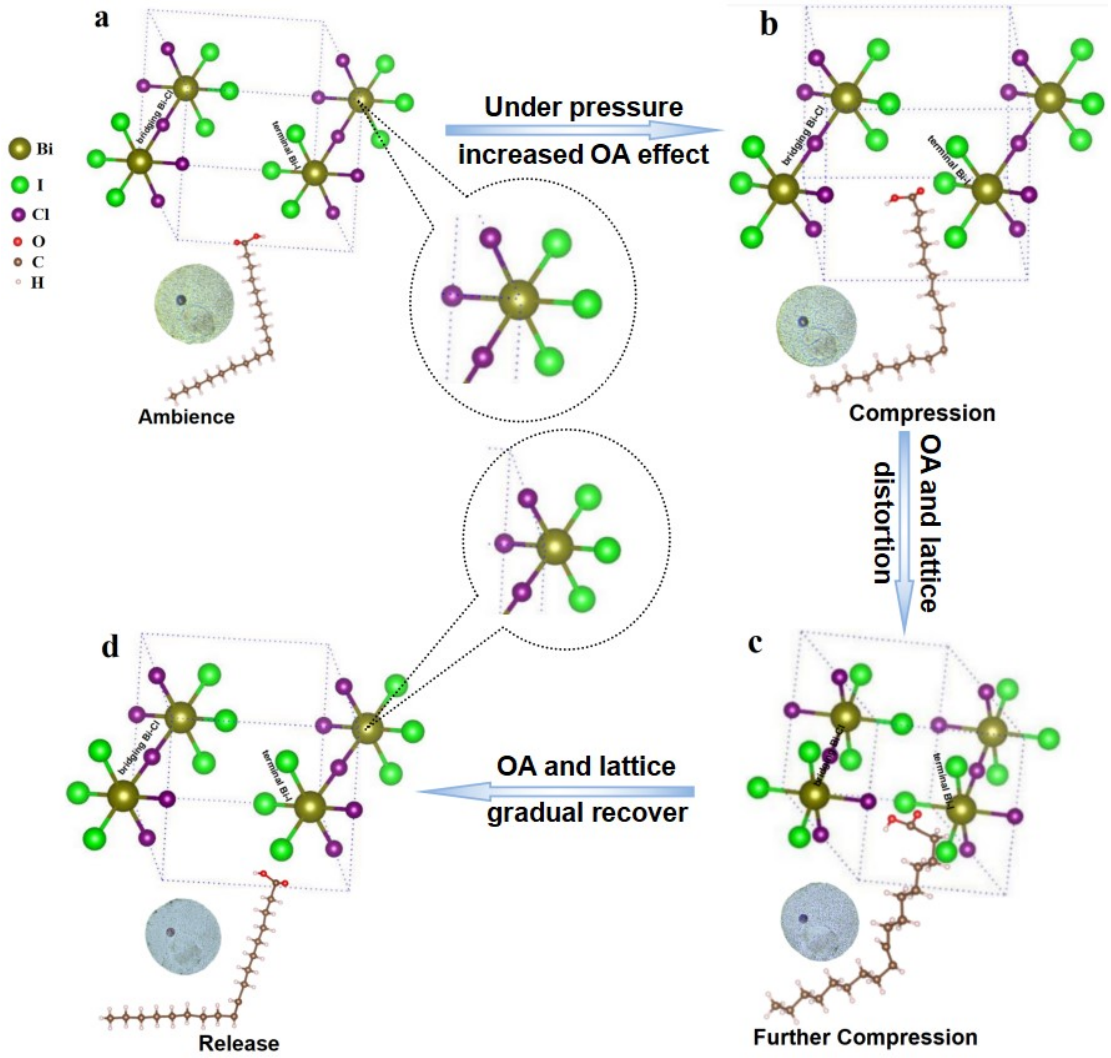

Figure S5. Schematic models of inorganic framework associated with Bi-Cl, Bi-I bonds and $[BiI_3Cl_3]^{3-}$ unit; the brown chain represents the OA molecule. The insets showed high pressure optical micrographs of $Cs_3Bi_2I_6Cl_3$ NCs in DAC.

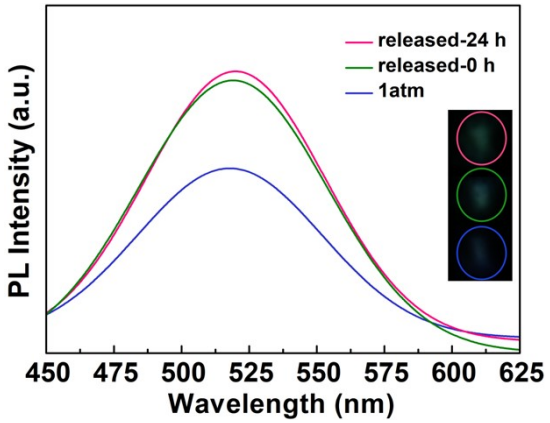

Figure S6. Time-dependent PL spectra of $Cs_3Bi_2I_6Cl_3$ NCs at 1 atm, complete pressure release, and pressure release with maintaining 24 h. Insets showed the corresponding PL micrographs.

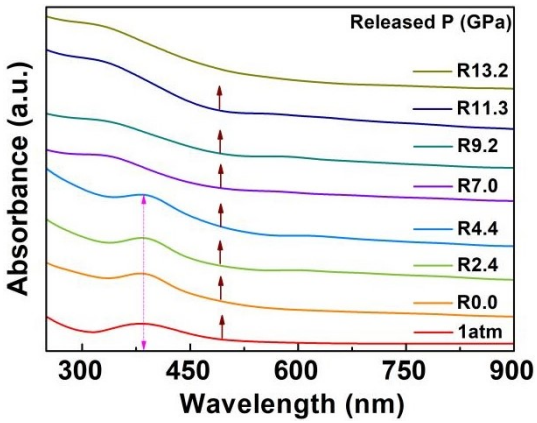

Figure S7. UV-vis absorption spectra of $Cs_3Bi_2I_6Cl_3$ NCs under decompression and ambient conditions for comparison. "R" represents absorption spectra collected on pressure release.

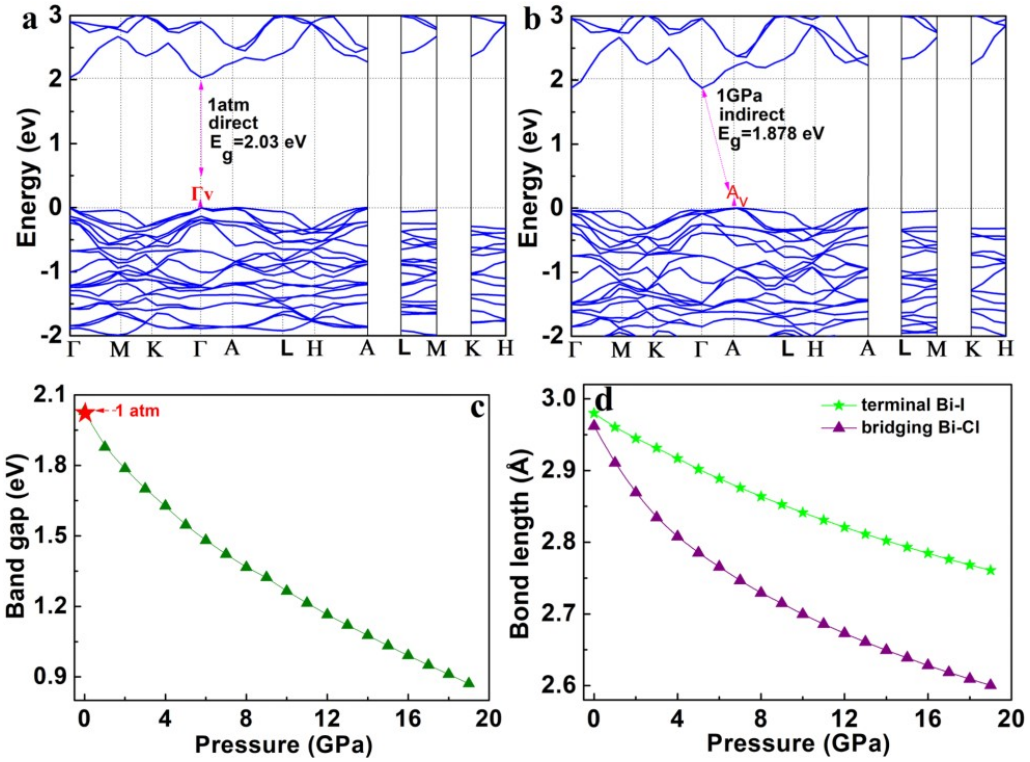

Figure S8. Calculated electronic band structure of $Cs_3Bi_2I_6Cl_3$ at ambient conditions (a) and 1 GPa (b), Calculated pressure-driven band gap (c) and bonds length evolution (d).

Table S1. Comparison of Raman Peaks of $Cs_3Bi_2I_9$/$Cs_3Bi_2I_6Cl_3$.

	Sample	Terminal Bi-I stretch (cm^{-1})	Bridge Bi-I stretch (cm^{-1})	Bridge Bi-Cl stretch (cm^{-1})	Ref
1	$Cs_3Bi_2I_9$ powder	146.6 127.2	104.5 90.0	/ /	[1]
2	$Cs_3Bi_2I_9$ powder	147.8 128.0	105.8 91.2	/ /	[2]
3	$Cs_3Bi_2I_6Cl_3$ powder	154 134	/ /	/ /	[3]
4	$Cs_3Bi_2I_6Cl_3$ NCs	142.7 125.5	/ /	101.8 /	[4]
5	$Cs_3Bi_2I_6Cl_3$ NCs	/ /	/ /	96.1 70.6	This work

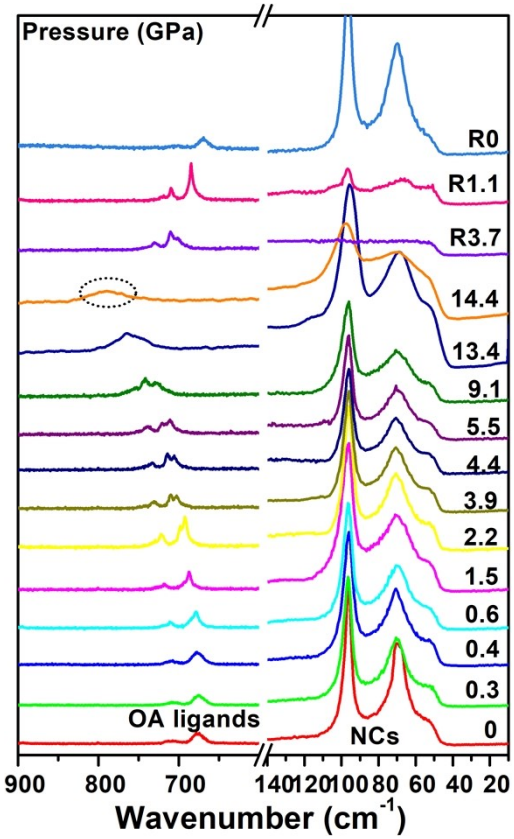

Figure S9. OA ligands Raman modes in $Cs_3Bi_2I_6Cl_3$ NCs under different pressure ranges.

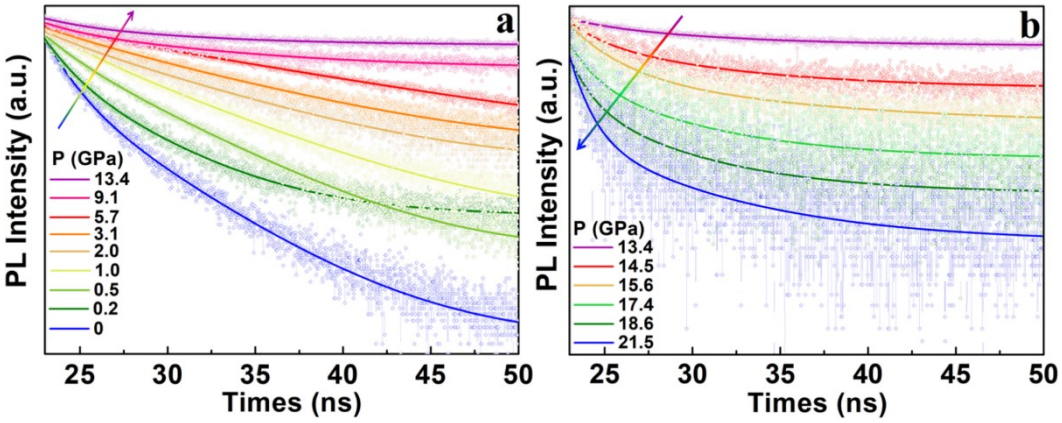

Figure S10. Time-resolved PL decay and fitting curves of $Cs_3Bi_2I_6Cl_3$ NCs under different pressure ranges.

Table S2. The fitting results of $Cs_3Bi_2I_6Cl_3$ NCs using a bi-exponential decay at different pressures.

sample	A_1	τ_1(ns) (ratio)(%)	A_2	τ_2 (ns) (ratio)(%)	τ_{avg} (ns)
1 atm	0.64	0.43 (78.7)	0.01	7.43 (21.3)	1.92
0.5 GPa	0.56	0.76 (62.2)	0.0298	8.67 (37.8)	3.75
1 GPa	0.65	0.79 (60.4)	0.0353	9.55 (39.6)	4.26
2 GPa	0.78	0.93 (56.3)	0.0831	8.55 (43.7)	4.70
3.1 GPa	0.80	1.27 (53.6)	0.0938	9.39 (46.4)	5.04
4.1 GPa	0.93	1.38 (50.9)	0.131	9.48 (49.1)	5.36
11.3 GPa	1.40	1.61 (39.2)	0.427	8.19 (60.8)	5.61
13.4 GPa	1.51	1.67 (34.5)	0.60	8.05 (65.5)	5.85
14.5 GPa	1.62	1.24 (36.1)	0.477	7.44 (63.9)	5.20
18.6 GPa	0.71	0.91 (44.8)	0.129	6.28 (55.2)	3.90
21.5 GPa	0.76	0.87 (46.2)	0.1361	5.65 (53.8)	3.44

Reference

[1] K. M. McCall, C. C. Stoumpos, S. S. Kostina, M. G. Kanatzidis, B. W. Wessels, Strong Electron–Phonon Coupling and Self Trapped Excitons in the Defect Halide Perovskites $A_3M_2I_9$ (A = Cs, Rb; M = Bi, Sb). *Chem. Mater.* **2017**, *29*, 4129-4145.

[2] L. Zhang, C. Liu, L. Wang, C. Kai, B. Zou, Pressure-Induced Emission Enhancement, Band Gap Narrowing and Metallization of Halide Perovskite $Cs_3Bi_2I_9$, *Angew. Chem. Int. Ed*. **2018**, *57*, 11213-11217.

[3] K. M. McCall, C. C. Stoumpos, O. Y. Kontsevoi, G. C. B. Alexander, B. W. Wessels, M. G. Kanatzidis, From 0D $Cs_3Bi_2I_9$ to 2D $Cs_3Bi_2I_6Cl_3$: Dimensional Expansion Induces Direct Bandgap but Enhances Electron-Phonon Coupling, *Chem. Mater*. **2019**, *31*, 2644-2650.

[4] K. Kundu, P. Acharyya, K. Maji, R, Sasmal, S. S. Agasti, K. Biswas, Synthesis and Localized Photoluminescence Blinking of Lead–Free 2D Nanostructures of $Cs_3Bi_2I_6Cl_3$ Perovskite, *Angew. Chem. Int. Ed*. **2020**, *59*, 13093-13100.